Progress In Electromagnetics Research M, Vol. 24, 179–192, 2012

THEORETICAL AND EXPERIMENTAL STUDIES OF 35 GHz AND 96 GHz ELECTROMAGNETIC WAVE PROPAGATION IN PLASMA

L. Zheng[1], Q. Zhao[1,*], S. Z. Liu[1], P. Ma[1], C. Huang[2], Y. F. Tang[1], X. L. Chen[1], X. J. Xing[1], C. Y. Zhang[1], and X. G. Luo[2]

[1]School of Physical Electronics, University of Electronic Science and Technology of China, Chengdu, China

[2]State Key Laboratory of Optical Technologies for Microfabrication, Institute of Optics and Electronics, Chinese Academy of Science, Chengdu, China

Abstract—The 35 GHz and 96 GHz electromagnetic wave propagation characteristics in plasma are studied theoretically and experimentally in this paper. The variations of the electromagnetic wave attenuation along with the plasma density, plasma collision frequency and electromagnetic wave frequency are acquired based on the physical model. The electromagnetic wave propagation properties in plasma are studied experimentally with the shock tube, and the experimental results match well with the theoretical ones. Both the theoretical and experimental results indicate that increasing the electromagnetic wave frequency is an alternative and effective method to solve the reentry blackout problem.

1. INTRODUCTION

The velocity of an spacecraft is very high, i.e., nearly several tens of times higher than the speed of sound, when the spacecraft reenters the Earth's atmosphere. The ultrahigh velocity results in the formation of a shockwave. Owing to the compression of the shockwave and the conglutination of the atmosphere, a part of the kinetic energy of the spacecraft changes into thermal energy. The temperature near the spacecraft may reach as high as 10000 to 12000 Kelvin, which lead

Received 7 March 2012, Accepted 19 April 2012, Scheduled 1 May 2012

* Corresponding author: Qing Zhao (zhaoq6666@163.com).

to the ionization of the surface materials and the ambient air. Then a plasma sheath is formed. The plasma sheath severely affects the propagation of the incident electromagnetic (EM) wave and causes severe EM wave attenuation, which results in the communication failures between the aircraft and the ground control center. Moreover, it will lead to the loss of radar targets and threaten the lives of the astronauts, which is known as "reentry blackout" and has attracted more and more attention recently [1–5]. Several solutions have been proposed to the problem, such as $\vec{E} \times \vec{B}$ cross-field configuration technology [1, 4], electrostatic plasma sheath technology [4], moving-window technology [2], magnetic window technology [5], etc.

In such a situation, it is important to study the properties of the EM wave propagation in plasma [6–8]. However, most of the published works focus on theories and numerical simulations [9–14] while few experimental studies on this issue have been carried out presently.

In this paper, the EM wave propagation characteristics in plasma are studied both theoretically and experimentally. The remainder of the paper is organized as follows: first of all, the physical model of the EM wave propagation in plasma is introduced. The simulation results of the EM wave propagation characteristics in plasma, including the effects of plasma density, plasma collision frequency and EM wave frequency on the reflectance, transmission and attenuation of the incidence EM wave, are exhibited and analyzed in Section 3. Then, the experimental studies of the EM wave propagation in plasma with the shock tube are presented. The conclusions of this paper are presented in Section 5.

2. PHYSICAL MODEL

The EM wave propagation properties are usually acquired by analyzing the permittivity of plasma [15–20]. The physical model used in this paper is as follows: the linearly polarized EM wave incident vertically into plasma along the negative z-axis, which is depicted in Figure 1. The plasma is assumed to be homogeneous, non-magnetized, steady-state and collisional. The electric field is parallel to y-axis, and the magnetic field is parallel to x-axis. The media are denoted by numbers: medium 0 (free space), medium 1 (plasma), and medium 2 (free space). The thickness of the plasma is d, which is set to 80 mm in the following numerical simulations. The multiple reflections occur at the interfaces $z = 0$ and $z = -d$.

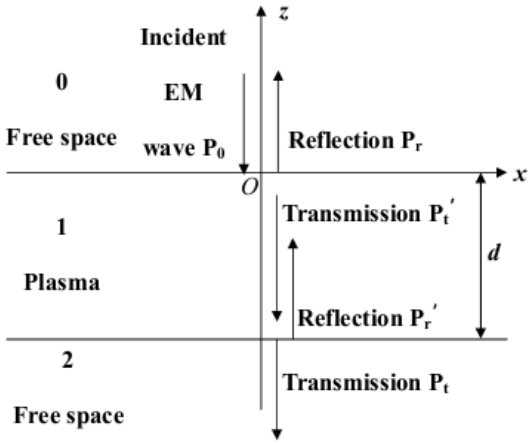

Figure 1. The physical model of the EM wave propagation in plasma.

The Maxwell's equations are as following [21, 22]:

$$\begin{cases} \nabla \times \vec{E} = -j\omega\mu_0\vec{H} \\ \nabla \times \vec{H} = j\omega\varepsilon\vec{E} \\ \nabla \cdot \left(\varepsilon\vec{E}\right) = 0 \\ \nabla \cdot \vec{B} = 0 \end{cases} \tag{1}$$

where $\vec{E}$ and $\vec{H}$ are the electric field and magnetic fields, respectively, μ_0 the permeability of the vacuum, ε the permittivity, $\omega = 2\pi f$, and f the frequency of the incident EM wave.

The electric field of the incident EM wave can be expressed as: $E_y = E_0 e^{jk_0 z}$, where E_0 is the amplitude of the incident electric field and k_0 the wave number in free space

From the Maxwell's equations, we can receive the magnetic field of the incident EM wave: $H_x = \frac{k_0}{\omega\mu_0} E_0 e^{jk_0 z}$.

Then the electric and magnetic fields in medium 0 can be expressed as

$$E_{0y} = E_0\left(e^{jk_0 z} + re^{-jk_0 z}\right) \qquad H_{0x} = \frac{k_0}{\omega\mu_0} E_0\left(e^{jk_0 z} - re^{-jk_0 z}\right) \tag{2}$$

where r is the reflection coefficient.

Similarly, the electric and magnetic fields in medium 1 are

expressed as

$$\begin{aligned} E_{1y} &= \left(E_{PT}e^{jk_pz} + E_{PR}e^{-jk_pz}\right) \\ H_{1x} &= \frac{k_p}{\omega\mu_0}\left(E_{PT}e^{jk_pz} - E_{PR}e^{-jk_pz}\right) \end{aligned} \tag{3}$$

where E_{PT} and E_{PR} are the amplitudes of the transmission and reflection electric fields in medium 1, and k_p is the wave number in plasma.

The electric and magnetic fields in medium 2 are presented as following:

$$E_{2y} = E_T e^{jk_0z} \qquad H_{2x} = \frac{k_0}{\omega\mu_0}E_T e^{jk_0z} \tag{4}$$

Here, E_T is the amplitude of the transmission electric field in medium 2.

The continuity boundary conditions of the electric and magnetic fields can be described as:

$$\begin{aligned} E_{0y}\,|_{z=0} &= E_{1y}\,|_{z=0} \\ H_{0x}\,|_{z=0} &= H_{1x}\,|_{z=0} \\ E_{1y}\,|_{z=-d} &= E_{2y}\,|_{z=-d} \\ H_{1x}\,|_{z=-d} &= H_{2x}\,|_{z=-d} \end{aligned} \tag{5}$$

i.e.,

$$\begin{aligned} &E_0\,(1+r) = E_{PT} + E_{PR} \\ &\frac{k_0}{\omega\mu_0}E_0\,(1-r) = \frac{k_p}{\omega\mu_0}\,(E_{PT} - E_{PR}) \\ &E_{PT}e^{-jk_pd} + E_{PR}e^{jk_pd} = E_T e^{-jk_pd} \\ &\frac{k_p}{\omega\mu_0}\left(E_{PT}e^{-jk_pd} - E_{PR}e^{jk_pd}\right) = \frac{k_0}{\omega\mu_0}E_T e^{-jk_0d} \end{aligned} \tag{6}$$

where r, E_{PT}, E_{PR} and E_T are unknown. The reflection coefficient r and transmission coefficient t can be obtained from Equation (6):

$$\begin{aligned} r &= \frac{1-\varepsilon_r}{2\sqrt{\varepsilon_r}\cot h(jk_pd) + \varepsilon_r + 1} \\ t &= \frac{E_T}{E_0} = \frac{2\sqrt{\varepsilon_r}e^{jk_0d}}{2\sqrt{\varepsilon_r}\cos h(jk_pd) + (\varepsilon_r+1)\sin h(jk_pd)} \end{aligned} \tag{7}$$

where ε_r is the relative permittivity of the plasma.

Then the reflectance, transmission and attenuation of the EM wave, i.e., R, T and Att, can be acquired and expressed as following:

$$R = |r|^2 \qquad T = |t|^2 \qquad Att = -10\log_{10}T \tag{8}$$

3. NUMERICAL SIMULATION RESULTS

3.1. The Effects of the Plasma Density on the EM Wave Propagation

The variations of the EM wave reflectance, transmission and attenuation along with the EM wave frequency and plasma density under fixed plasma collision frequency are obtained based on the physical model and theoretical analysis, depicted in Figure 2, Figure 3 and Figure 4, respectively.

Figure 2 shows the variations of the EM wave reflectance along with the EM wave frequency and plasma density. We can see that the EM wave reflectance decreases in general with increasing EM wave frequency for identical plasma collision frequency and plasma density. Furthermore, it can be seen that the EM wave reflectance increases with increasing plasma density for identical plasma collision frequency and EM wave frequency. The EM wave reflectance increases by two

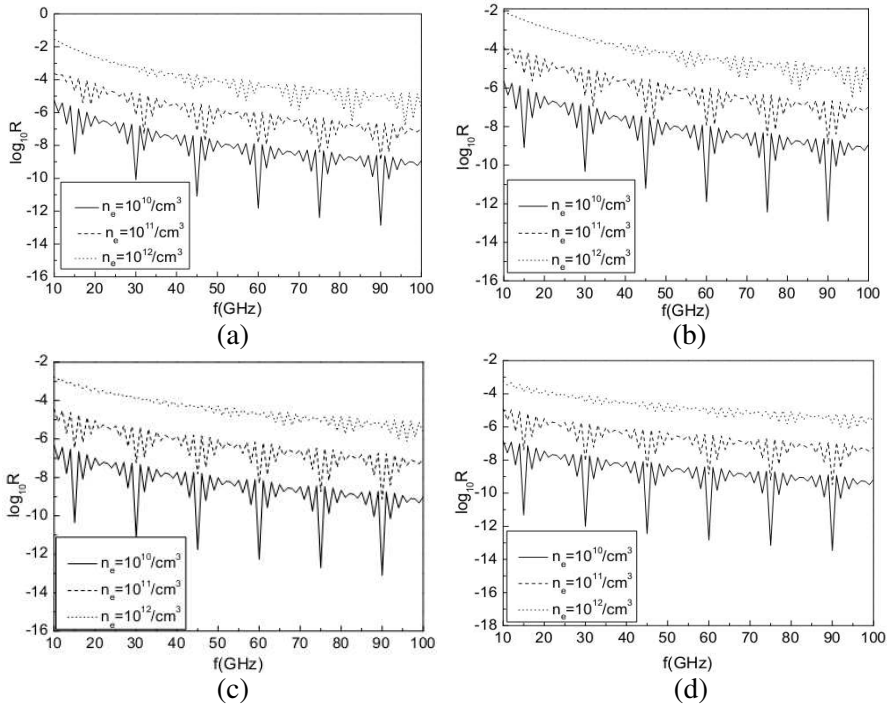

Figure 2. The variations of the EM wave reflectance along with the EM wave frequency and plasma density. (a) $f_{en} = 10\,\text{GHz}$. (b) $f_{en} = 20\,\text{GHz}$. (c) $f_{en} = 50\,\text{GHz}$. (d) $f_{en} = 90\,\text{GHz}$.

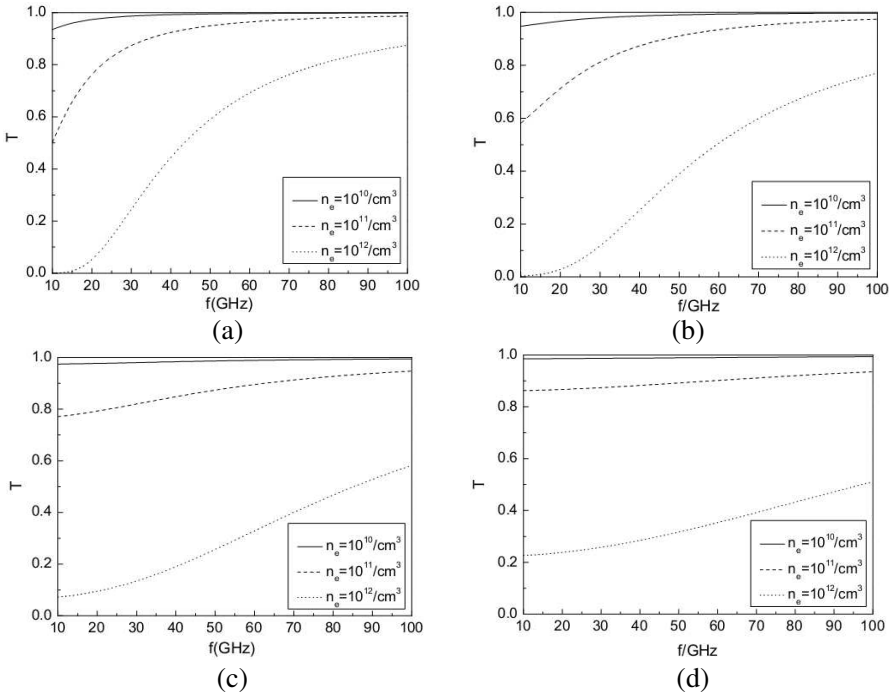

Figure 3. The variations of the EM wave transmission along with the EM wave frequency and plasma density. (a) $f_{en} = 10\,\mathrm{GHz}$. (b) $f_{en} = 20\,\mathrm{GHz}$, (c) $f_{en} = 50\,\mathrm{GHz}$, (d) $f_{en} = 90\,\mathrm{GHz}$.

orders of magnitude with the plasma density increases by one order of magnitude. Moreover, there are several valleys on the reflectance curves, and the values of the valleys decrease while the corresponding EM wave frequency increases with increasing plasma density. The phenomenon is owing to the cavity resonance effects; however, the effects of the plasma density on the resonance was not described by Yuan et al. [15]. The cavity resonance has a more obvious effect on the EM wave reflectance for higher EM wave frequency, while the effect becomes less obvious for higher plasma density. In essence, the cavity resonance effect is attributed to the multiple EM wave reflections at the interfaces $z = 0$ and $z = -d$.

The EM wave transmission increases and attenuation decreases with increasing EM wave frequency for identical plasma collision frequency and plasma density, which are presented meticulously in Figure 3 and Figure 4. The mechanism responsible for this phenomenon is complicated and can be explained through the electrons' response to the electric field. Under higher EM wave

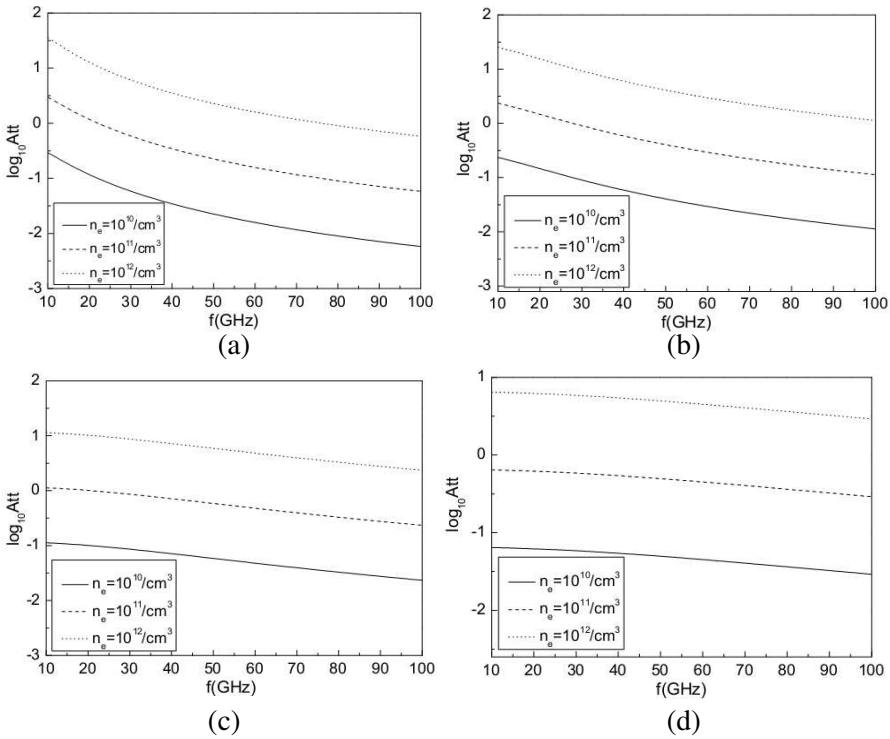

Figure 4. The variations of the EM wave attenuation along with the EM wave frequency and plasma density. (a) $f_{en} = 10\,\text{GHz}$. (b) $f_{en} = 20\,\text{GHz}$. (c) $f_{en} = 50\,\text{GHz}$. (d) $f_{en} = 90\,\text{GHz}$.

frequency, the electrons will no longer be able to response to the electric field, hence, the EM wave energy absorbed by the electrons is decreased, and the attenuation of the EM wave will be decreased.

In Figure 3 and Figure 4, we can also find that the EM wave transmission decreases and attenuation increases with increasing plasma density for identical plasma collision frequency and EM wave frequency. Moreover, the EM wave attenuation increases by one order of magnitude with plasma density increasing an order of magnitude, because with higher plasma density, there are more electrons in the plasma, and more EM energy is absorbed by the electrons and passed to neutral particles through collisions, i.e., the EM wave attenuation in the plasma is increased.

3.2. The Effects of the Plasma Collision Frequency on the EM Wave Propagation

The variations of the EM wave reflectance, transmission and attenuation along with the EM wave frequency and plasma collision frequency under fixed plasma density are obtained based on the physical model and theoretical analysis, shown in Figure 5, Figure 6 and Figure 7, respectively.

Figure 5 shows the variations of the EM wave reflectance along with the EM wave frequency and plasma collision frequency. We can see that the EM wave reflectance decreases in general with increasing EM wave frequency for identical plasma density and plasma collision frequency. Moreover, the EM wave reflectance decreases with increasing plasma collision frequency under identical plasma density and EM wave frequency. The cavity resonance effects are also involved in these conditions.

The EM wave transmission increases and attenuation decreases with increasing EM wave frequency under identical plasma density and

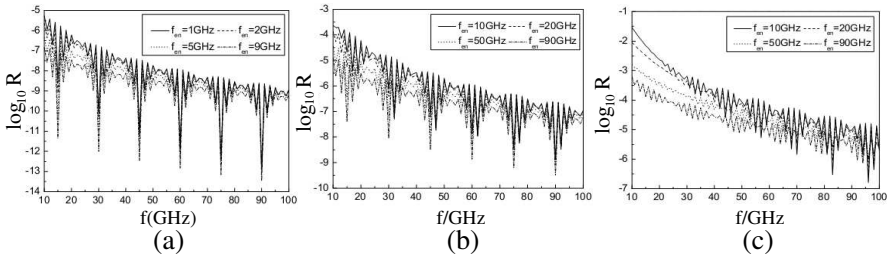

Figure 5. The variations of the EM wave reflectance along with the EM wave frequency and plasma collision frequency. (a) $n_e = 10^{10}/\text{cm}^3$. (b) $n_e = 10^{11}/\text{cm}^3$. (c) $n_e = 10^{12}/\text{cm}^3$.

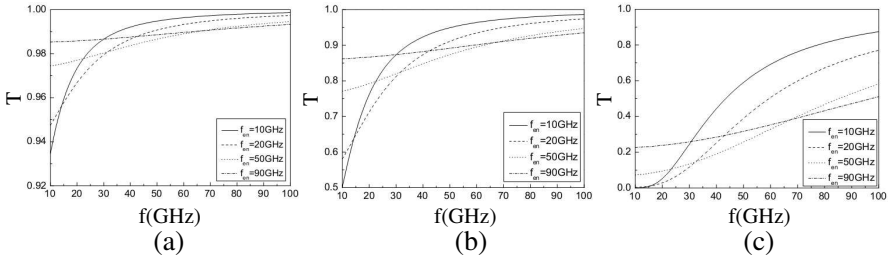

Figure 6. The variations of the EM wave transmission along with the EM wave frequency and plasma collision frequency. (a) $n_e = 10^{10}/\text{cm}^3$. (b) $n_e = 10^{11}/\text{cm}^3$. (c) $n_e = 10^{12}/\text{cm}^3$.

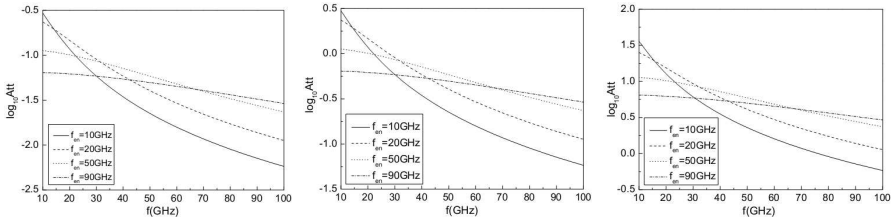

Figure 7. The variations of the EM wave attenuation along with the EM wave frequency and plasma collision frequency. (a) $n_e = 10^{10}/\text{cm}^3$. (b) $n_e = 10^{11}/\text{cm}^3$. (c) $n_e = 10^{12}/\text{cm}^3$.

plasma collision frequency, which can be seen in Figure 6 and Figure 7. The reasons have been given in the previous section.

In Figure 6 and Figure 7, we can also find that the EM wave transmission first decreases and then increases, while the attenuation first increases and then decreases with increasing plasma collision frequency for identical plasma density and EM wave frequency. The performance of the incident EM wave can be explained through the effects of the plasma collision frequency: under higher plasma collision frequency, the collision probability between the electrons and neutral particles increases, and the energy passed to the neutral particles is increased, then the attenuation of the incident EM wave increases. However, when the collision frequency is too high, the acceleration time of the electrons before collision with the neutral particles is so short that there is little time for the electron to receive energy from the electric filed, so the attenuation decreases on the contrary.

4. EXPERIMENTAL RESULTS

The EM wave propagation properties in plasma are studied experimentally with a shock tube. The shock tube is a cylindrical device and can produce approximately uniform plasma, which can be used to simulate the plasma near the aircrafts for simplification. The schematic diagram of the experimental setup is shown in Figure 8. The diameter of the shock tube is 80 mm. The absorbing materials were set around the antennas, and the test section of the original shock tube wall was replaced by Teflon in order to reduce reflection. The 35 GHz and 96 GHz experimental systems were used to measure the attenuation of plasma at the same time. The theoretical EM wave attenuation is achieved based on the physical model in Section 2, and the experimental EM wave attenuation is acquired from the power of

the receiver and can be obtained from the "Data processing system". A total of nine effective experiments were carried out, and we denote the experiments by numbers: 1, 2, 3, . . . , 9. The plasma densities and collision frequencies used in the experiments are presented in Table 1, which are calculated based on the physical states of the shock tube in the experiments.

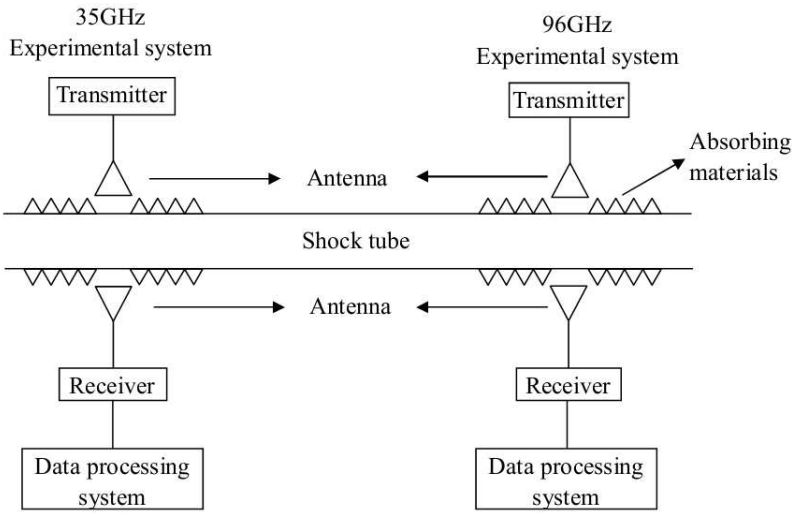

Figure 8. The experimental setup of the EM wave propagation in plasma.

Table 1. The plasma densities and collision frequencies used in the experiments.

Number of the experiments	n_e **(cm**$^{-3}$**)**	f_{en} **(Hz)**
1	5.0×10^{10}	4.0×10^{10}
2	5.9×10^{10}	4.0×10^{10}
3	7.3×10^{10}	4.2×10^{10}
4	1.6×10^{11}	6.1×10^{10}
5	4.0×10^{11}	4.1×10^{10}
6	6.0×10^{11}	4.0×10^{10}
7	9.0×10^{11}	5.7×10^{10}
8	1.5×10^{12}	4.2×10^{10}
9	6.9×10^{12}	9.7×10^{10}

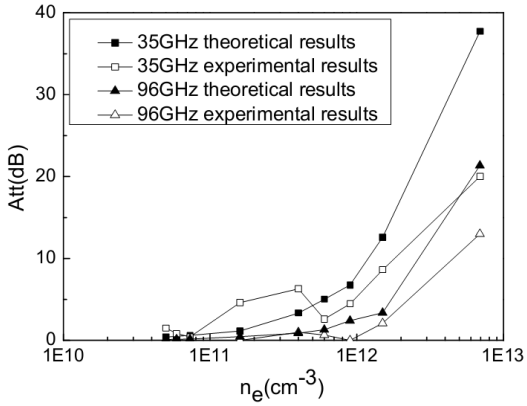

Figure 9. The comparison of the experimental and theoretical EM wave attenuation at 35 GHz and 96 GHz.

Figure 9 shows the comparison of the experimental and theoretical EM wave attenuations at 35 GHz and 96 GHz. The theoretical and experimental EM wave attenuations at 35 GHz are both larger than those at 96 GHz. Thus, it can be deduced that increasing the EM wave frequency is an alternative and effective method to solve the reentry blackout problems.

The experimental results match well with the theoretical ones, which can also be seen from Figure 9. However, there are some differences between the experimental and theoretical results, which may be attributed to the errors of the experimental systems or the calculation errors of the plasma densities and collision frequencies. The EM wave propagation characteristics are strongly affected by plasma density and collision frequency. For example, the EM wave attenuation increases by one order of magnitude with plasma density increasing an order of magnitude. According to these reasons, the differences between the experimental and theoretical results are reasonable and understandable.

5. CONCLUSIONS

The EM wave propagation characteristics in plasma at 35 GHz and 96 GHz are studied theoretically and experimentally in this paper. The variations of the EM wave attenuation along with the plasma density, collision frequency and EM wave frequency are acquired: (1) the EM wave attenuation increases by one order of magnitude with the plasma density increases an order of magnitude; (2) the EM wave attenuation first increases and then decreases with increasing plasma collision

frequency; (3) the EM wave attenuation decreases with increasing EM wave frequency. The EM wave propagation properties in plasma are studied experimentally with the shock tube, and the experimental results match well with the theoretical ones. Both the theoretical and experimental results indicate that increasing the EM wave frequency is an alternative and effective method to solve the reentry blackout problem.

ACKNOWLEDGMENT

This work was supported by the National Basic Research Program of China under Grant No. 2011CB301805, the International Cooperation Projects under Grant No. OS2012R0151, the National High Technology Research and Development Program of China under Grant No. 2011AA7022016 and the Foundation of the State Key Laboratory of Optical Technologies for Microfabrication under Grant No. M160104012011E11.

REFERENCES

1. Keidar, M., "Electromagnetic reduction of plasma density during atmospheric reentry and hypersonic flights," *Journal of Spacecraft and Rockets*, Vol. 45, 445–453, 2008.
2. Liu, J. F., X. L. Xi, G. B. Wan, and L. L. Wang, "Simulation of electromagnetic wave propagation through plasma sheath using the moving-window finite-difference time-domain method," *IEEE Transactions on Plasma Science*, Vol. 39, 852–855, 2011.
3. Ma, C. G., Q. Zhao, X. G. Luo, G. He, L. Zheng, and J. W. Liu, "Study on attenuation characteristics of millimeter wave in plasma," *Acta Physica Sinica*, Vol. 60, 055201, 2010.
4. Kim, M., M. Keidar, and I. D. Boyd, "Analysis of an electromagnetic mitigation scheme for reentry telemetry through plasma," *Journal of Spacecraft and Rockets*, Vol. 45, 1223–1229, 2008.
5. Thoma, C., D. V. Rose, C. L. Miller, R. E. Clark, and T. P. Hughes, "Electromagnetic wave propagation through an overdense magnetized collisional plasma layer," *Journal of Applied Physics*, Vol. 106, 043301, 2009.
6. Ai, X., Y. Han, C. Y. Li, and X. W. Shi, "Analysis of dispersion relation of piecewise linear recursive convolution FDTD method for space-varying plasma," *Progress In Electromagnetics Research Letters*, Vol. 22, 83–93, 2011.

7. Yin, X., H. Zhang, H. Y. Xu, and X. F. Zeng, "Improved shift-operator FDTD method for anisotropic magnetized cold plasmas with arbitrary magnetic field declination," *Progress In Electromagnetic Research B*, Vol. 38, 39–56, 2012.
8. Gurel, C. S. and E. Oncu, "Characteristics of electromagnetic wave propagation through a magnetized plasma slab with linearly varying electron density," *Progress In Electromagnetics Research B*, Vol. 21, 385–398, 2010.
9. Cheng, G. X. and L. Liu, "Direct finite-difference analysis of the electromagnetic-wave propagation in inhomogeneous plasma," *IEEE Transactions on Plasma Science*, Vol. 38, 3109–3115, 2010.
10. Yang, H. W. and R. S. Chen, "FDTD analysis on the effect of plasma parameters on the reflection coefficient of the electromagnetic wave," *Opt. Quant. Electron.*, Vol. 39, 1245–1252, 2007.
11. Liu, S. B., J. J. Mo, and N. C. Yuan, "FDTD analysis of electromagnetic reflection by conductive plane covered with magnetized inhomogeneous plasmas," *International Journal of Infrared and Millimeter Waves*, Vol. 23, 1803–1815, 2002.
12. Tang, D. L., A. P. Sun, X. M. Qiu, and P. K. Chu, "Interaction of electromagnetic waves with a magnetized nonuniform plasma slab," *IEEE Transactions on Plasma Science*, Vol. 31, 405–410, 2003.
13. Angus, J. R., S. I. Krasheninnikov, and A. I. Smolyakov, "Kinetic theory of electromagnetic plane wave obliquely incident on bounded plasma slab," *Physics of Plasma*, Vol. 17, 102115, 2010.
14. Brodin, G., M. Marklund, L. Stenflo, and P. K. Shukla, "Dispersion relation for electromagnetic wave propagation in a strongly magnetized plasma," *New Journal of Physics*, Vol. 8, 1–6, 2008.
15. Yuan, C. X., Z. X. Zhou, and H. G. Sun, "Reflection properties of electromagnetic wave in a bounded plasma slab," *IEEE Transactions on Plasma Science*, Vol. 38, 3348–3355, 2010.
16. Ma, L. X., H. Zhang, and C. X. Zhang, "Analysis on the reflection characteristic of electromagnetic wave incidence in closed nonmagnetic plasma," *Journal of Electromagnetic Waves and Applications*, Vol. 22, Nos. 17–18, 2285–2296, 2008.
17. Nishimoto, M. and H. Ikuno, "Time-frequency analysis of electromagnetic pulse response from a one-dimensional plasma medium," *Journal of Electromagnetic Waves and Applications*, Vol. 18, No. 2, 181–196, 2004.

18. Yang, H. W., W. C. Tang, and X. K. Kong, "Calculation of the effect on the reflection of the plane electromagnetic wave for non-magnetized plasma with different electron density distributions," *International Journal of Infrared and Millimeter Waves*, Vol. 28, 547–556, 2007.
19. Chaudhury, B. and S. Chaturvedi, "Comparison of wave propagation studies in plasmas using three-dimensional finite-difference time-domain and ray-tracing methods," *Physics of Plasmas*, Vol. 13, 123302, 2006.
20. Shi, J. M., J. C. Wang, Z. C. Yuan, and Y. S. Ling, "Electromagnetic reflection of conductive plane covered with magnetized inhomogeneous plasma," *Internal Journal of Infrared and Millimeter Waves*, Vol. 22, 1167–1175, 2001.
21. Yuan, C. X., Z. X. Zhou, X. L. Xiang, H. G. Sun, and S. Z. Pu, "Propagation of broadband terahertz pulses through a dense-magnetized-collisional-bounded plasma layer," *Physics of Plasmas*, Vol. 17, 113304, 2010.
22. Yuan, C. X., Z. X. Zhou, and X. L. Xiang, "Properties of terahertz waves propagation in a bounded plasma slab with high collision frequency and high density," *International Conference on Optoelectronics and Image Processing*, Haiko, China, Nov. 2010.